ISET Journal of Earthquake Technology, Paper No. 520, Vol. 49, No. 1-2, March-June 2012, pp. 37–52

EFFECT OF SEISMIC OBLIQUE WAVES ON DYNAMIC RESPONSE OF AN EMBEDDED FOUNDATION

Salah Messioud*, Badreddine Sbartai** and Daniel Dias***
*Department of Civil Engineering, University of Jijel, 18000 Jijel, Algeria
**Department of Civil Engineering, University of Skikda, 21000 Skikda, Algeria
***Department of Geotechnical and Civil Engineering, Polytech Grenoble, 38400 Saint-Martin-d'Hères, France

ABSTRACT

This study analyzes the influence of soil-structure interaction on the seismic response of a three-dimensional (3-D) rigid foundation on the surface of a viscoelastic soil limited by bedrock. The vibrations are assumed to result only from the P, SV, SH and R harmonic seismic waves. The key step here is the characterization of the soil-foundation interaction with the impedance matrix on one hand and input motion matrix on the other hand. The mathematical approach is based on the method of integral equations in the frequency domain using the formalism of Green's functions for a layered soil. This approach is applied to analyze the effect of soil-structure interaction on the seismic response of the foundation as a function of the kind of incident wave, angle of wave incidence, wave frequency and embedment of foundation.

KEYWORDS: Wave Propagation, BEM-TLM Method, Soil-Structure Interaction

INTRODUCTION

The analysis of the behavior of foundations under dynamic loads has grown considerably over the past four decades. Stringent security requirements imposed on the design of certain types of structures have played an important role in the development of analytical methods. The key step in studying the dynamic response of foundations is the determination of the relationship between various forces. This relationship, which results in displacements, is expressed by using impedance functions (i.e., dynamic stiffnesses) or compliance functions (i.e., dynamic flexibilities). The consideration of the soil-structure interaction in the analysis of the dynamic behaviour of foundations allows us to realistically take into account the influence of soils on their vibrations.

A myriad of methods have been proposed to solve the problem of soil-structure interaction. To simplify the problem, various linear-analysis techniques have been developed. One of the most commonly used approaches is the substructuring method that allows the problem to be analyzed in two parts (Aubry and Clouteau, 1992; Kausel et al., 1978; Pecker, 1984). In this approach the dynamic response of superstructure elements and substructure are examined separately. The analysis of the foundation system can be reduced to the study of dynamic stiffnesses at the soil-foundation interface (known as impedance functions) and driving forces from the incident waves. The kinematic interaction of the foundation with the incident waves is implemented in the form of a driving-force vector.

The determination of foundation response is a wave propagation problem. Due to the mixed-boundary conditions of the problem (i.e., displacement compatibility with the stress distribution underneath the foundation and zero tension outside), the solutions are complex. The determination of impedance functions and forces of movement related to the incident waves is a complex process. Several studies have been conducted on the dynamic response of foundations by using the finite-element and boundary-element methods. Wong and Luco (1978) have shown the importance of the effect of the non-verticality of SV and SH harmonics on the response of a foundation.

Apsel and Luco (1987) used an integral-equation approach based on Green's functions for multilayered soils to calculate the impedance functions of a foundation. Using this approach, Wong and Luco (1986) studied the dynamic interaction between the rigid foundations resting on half-space. Boumekik (1985) studied the problem of 3-D foundations embedded in the soil limited by a rigid substratum. The finite-element method was applied by Kausel et al. (1978), Kausel and Roësset (1981), and Lin and Tassoulas (1986) to determine the behavior of rigid foundations placed on or embedded in a soil layer limited by a rigid substratum. A formulation of the boundary-element method in the frequency domain has also been developed to address the wave-propagation problems of soil-structure interaction and structure-soil-structure interaction, which limits discretization at the interface of soil and foundation. In this approach, the displacement field is formulated as an integral equation in terms of Green's functions (Beskos, 1987; Aubry and Clouteau, 1992; Qian and Beskos, 1996; Karabalis and Mohammadi, 1998; Mohammadi, 1992). Çelebi et al. (2006) used the boundary-element method with integral formulation (i.e., BIEM) to compute the dynamic impedance of foundations. In this context, the analytical solutions of 3-D wave equations in cylindrical coordinates in a layered medium, while satisfying the necessary boundary conditions, have been employed by Liou (1993) and Liou and Chung (2009). Sbartai and Boumekik (2008) used the BEM-TLM method to calculate the dynamic impedance of rectangular foundations placed or embedded in a layered soil limited by a substratum and also the propagation of vibrations in the vicinity of a vibrating foundation. They further used the BEM-TLM method to analyze the effects of some parameters on the dynamic response of those foundations. These parameters are the depth of the substratum, embedment, masses and shape of the foundation, soil heterogeneity, and frequency. However, Sbartai and Boumekik (2006, 2007) have studied the dynamic response of two square foundations placed or embedded in a layered soil limited by a substratum. Spryakos and Xu (2004) have developed a hybrid BEM-FEM method and have conducted several studies for the parametric analysis of soil-structure interaction.

Recently, McKay (2009) used the reciprocity theorem based on the BIEM to analyze the influence of soil-structure interaction on the seismic response of foundations. Suárez et al. (2002) applied the BIEM to determine the seismic response of an L-shaped foundation. In addition, experimental work has been carried out by researchers in Japan to determine the effect of soil-structure interaction on the response of real structures (Fujimori et al., 1992; Ohtsuka et al., 1996; Mizuhata et al., 1988; Watakabe et al., 1992; Imamura et al., 1992).

In the present study, a solution is derived from the boundary element method (BEM) in the frequency domain with constant quadrilateral elements and the thin-layer method is used to analyze the influence of soil-structure interaction on the response of seismic foundations. The results are presented as the coefficients of movement in the matrix $\left[S^*\right]$ and in terms of displacement as a function of dimensionless frequency, angles of incidence (vertically and horizontally) and embedment of foundation. This paper is in continuation of the work published in Sbartai and Boumekik (2008) where the impedance functions have been well studied in detail. Therefore, those impedance functions are not discussed in this paper.

FOUNDATION RESPONSE TO WAVES OF SEISMIC ORIGIN

1. Physical Model and Basic Equations

The geometry of the calculation model is shown in Figure 1. We consider a 3-D, rigid, massless, surface foundation of an arbitrary shape S in full contact with a homogeneous, isotropic and linearly-elastic soil that is limited by a bedrock. The soil is characterized by its density ρ, shear modulus G, damping coefficient β and Poisson's ratio ν. The foundation is subjected to the harmonic oblique-incident waves that are time-dependent, i.e., P, SV, SH and R.

The movement of an arbitrary point ζ can be obtained by solving the wave equation:

$$\left(C_P^2 - C_S^2\right)u_{j,ij} + C_S^2\, u_{i,jj} - \omega^2 u_i = 0 \qquad (1)$$

where C_S and C_P are the velocities of shear and compression waves respectively and ω the angular frequency of excitation. Further, u_i is the component of the harmonic displacement vector in the x-direction; $u_{j,ij}$ is the partial derivative of the displacement field with respect to x and y; and $u_{i,jj}$ is the second partial derivative of the displacement field with respect to y. The solution of Equation (1) may be expressed by the following integral equation:

$$u_j\left(x,\omega\right) = \int_S G_{ij}\left(x,\xi,\omega\right) t_i\left(\xi,\omega\right) \mathrm{d}s\left(\xi\right) \qquad (2)$$

with G_{ij} denoting Green's functions at the point i due to unit harmonic loads (vertical and horizontal) on the ground at the point j, and t_i being the load (i.e., traction) distributed over an area of the soil.

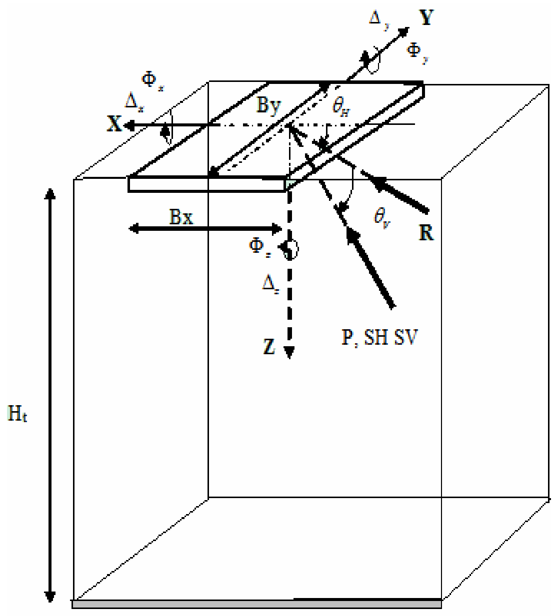

Fig. 1 Geometry of foundation subjected to harmonic seismic waves

The medium is continuous and, therefore, the relationship in Equation (2) is very difficult to solve. However, if the soil mass is discretized appropriately, this relationship can be made algebraic and displacements can be calculated. The key step of this study is to determine the impedance matrix linking the harmonic forces applied with the resulting harmonic displacements. Even with a continuous medium, the determination of the impedance matrix is very difficult, if not impossible, due to the propagation problem and mixed-boundary conditions. However, if the medium is discretized both vertically and horizontally, it is possible to make the problem algebraic by considering the variation of interface displacement to be a linear function. The principle of horizontal and vertical discretizations of the soil mass is shown in Figure 2, where H_t denotes the height of the soil mass, h_1 the height of the sublayer 1, N_x the number of elements in the x-direction for a horizontal plane, N_y the number of elements in the y-direction for a horizontal plane, N_z the number of soil layers, N the total number of elements in the soil-foundation interface, and B_x and B_y the dimensions of the foundation. The principle of vertical discretization is based on the division of every soil layer into a number of sublayers of height h_j with similar physical characteristics. Each sublayer is assumed to be horizontal, viscoelastic, and isotropic, and is characterized by the Lame constant λ_j, shear modulus μ_i and density ρ_j. The bedrock at the depth H_t is considered infinitely rigid and is not discretized. The reflected wave is assumed to be total and the displacements null.

Within a given sublayer, the displacement is assumed to be a linear function of the interface displacements above and below. This is true when the height of the sublayer is small in relation to the wavelength considered (in the order of $\lambda/10$). This method is comparable to the FEM in the sense that the movements within each sublayer are completely defined from the displacements in the middle of the interfaces. The interaction between the elements is done only through their nodes. The degrees of freedom of the soil mass are thus reduced to the degrees of freedom of the nodes. The stiffness matrix of the soil mass is obtained in a manner similar to how it is determined in the FEM. This technique developed by Lysmer and Waas (1972) is known as the thin-layer method (TLM) and used mainly for horizontal soil layers. This method has the advantage of making the problem algebraic and thus obtains Green's functions by applying the BEM on the soil-foundation interface. For this reason, a horizontal discretization of the soil-foundation interface is established.

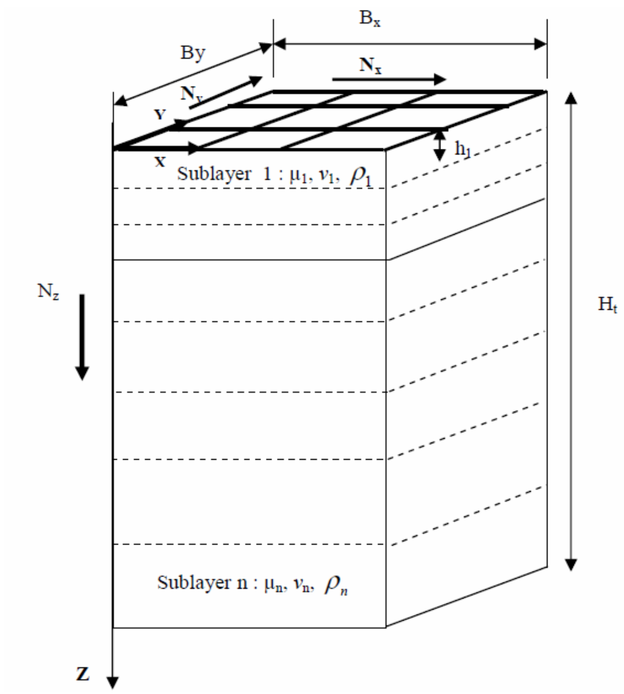

Fig. 2 Model of calculation

The horizontal discretization permits a subdivision of any horizontal soil-foundation interface by the elements of square sections, S_k. The constant-moving average is replaced by the movement of the center in these elements as shown in Figure 2 and it is assumed that stress distribution is uniform in these elements. For the sake of simplicity in integration calculations and economy in computational time, the square elements are approximated as disc elements. If unit loads are applied to the disc j (along the directions x, y, z), Green's functions at the center of the disc i can be determined. By successively applying these loads on all the discs, the flexibility matrix of the soil mass at a given frequency ω can be formed. The discretized model to calculate the impedance functions of the foundation is also presented in Figure 2. In this model, Equation (2) is expressed in an algebraic form as follows:

$$u_j = \sum_{i=1}^{N} \int_S G_{ij} t_i \mathrm{d}s \tag{3}$$

2. Determination of Green's Functions by TLM

Green's functions for a layered stratum are obtained by an inversion of the thin-layer stiffness matrix by using spectral-decomposition procedure by Kausel and Peek (1982). The advantage of the thin-layer-stiffness matrix technique over the classical transfer-matrix technique for finite layers and the finite-layer-stiffness matrix technique (Kausel and Roësset, 1981) is that the transcendental functions in the layered-stiffness matrix are linearized.

In this work, the body B represents a layered stratum resting on a substratum base with n horizontal layer interfaces defined by $z = z_1, z_2, ..., z_n$ and with the layer j defined by $z_n < z < z_{n+1}$, as shown in Figure 3. The medium of the nth layer of thickness h_n is assumed to be homogeneous, isotropic, and linearly elastic. For the body B, Green's functions in frequency domain are obtained with the help of the TLM. According to the thin-layer theory of Lisper and Waas (1972), displacements in each sublayer vary linearly from one plane to another while continuing in the relevant direction x, y or z. Thus, the displacements in each sublayer are obtained by the linear interpolation of nodal displacements at the interface of the sublayer n as follows:

$$U^{(n)}(z) = (1-\eta)U^n + \eta U^{n+1} \tag{4a}$$

$$V^{(n)}(z) = (1-\eta)V^n + \eta V^{n+1} \tag{4b}$$

$$W^{(n)}(z) = (1-\eta)W^n + \eta W^{n+1} \tag{4c}$$

where $\eta = (z - z_n)/h_n$ with $0 \le \eta \le 1$. Further, $U^{(n)}$, $V^{(n)}$ and $W^{(n)}$ are the displacements along the x-, y- and z-axes as the functions of z in the layer j, and U^n, V^n and W^n are their nodal values respectively at the interface layer $z = z_n$. Green's functions are obtained as

$$G_{ij}^{mn} = \sum_{l=1}^{2N} \frac{a_{\alpha\beta}\varphi_i^{ml}\varphi_j^{nl}}{k^2 - k_l^2} \tag{5}$$

with $a_{\alpha\beta} = 1$, if $\alpha = \beta$; $a_{\alpha\beta} = k/k_l$, if $\alpha \ne \beta$; and $i, j = x, y, z$. Further, k and k_l represent the wave numbers, m represents the interface where the load is applied, and n represents the interface where Green's functions are calculated.

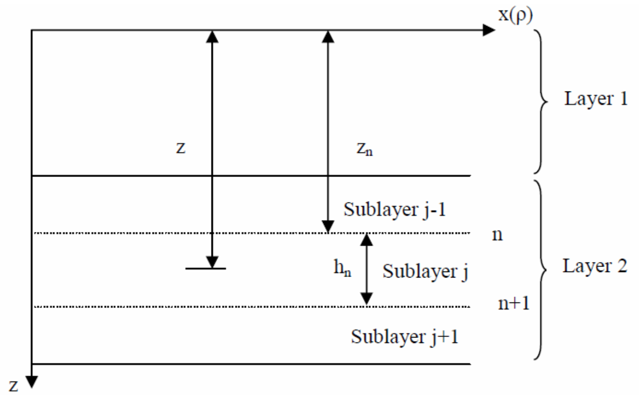

Fig. 3 Geometry of soil layers represented by body *B*

Green's functions so obtained are complex and constitute the starting point for the determination of the flexibility matrix of an arbitrary soil volume. However, on considering the geometry of the foundation, a system of Cartesian coordinates is adopted. The above expressions of U, V, W and Green's functions are in fact the terms of the flexibility matrix of the soil. The determination of this flexibility matrix gives the impedance functions of one or several foundations and the amplitudes of vibrations in the neighborhood of a foundation (Sbartai and Boumekik, 2007, 2008).

The viscoelastic soil behavior is easily introduced in the above formulation by simply replacing the elastic constants λ and G with their complex values,

$$\lambda^*(Z) = \lambda(1 + 2i\beta) \tag{6a}$$

$$\mu^*(Z) = \mu(1 + 2i\beta) \tag{6b}$$

respectively, where β is the hysteretic damping coefficient.

CALCULATION MODEL

The total displacement matrix of the soil is obtained by a successive application of unit loads on the constituents of the discretized solid ground. The displacements in the soil are then expressed as

$$\{u\} = [G]\{t\} \tag{7}$$

where the vectors $\{u\}$ and $\{t\}$ denote the nodal values of the amplitudes of displacements and tractions respectively at the soil-foundation interface, and $[G]$ denotes the flexibility matrix of the soil.

When the foundation is in place, it requires different components of soil displacements consistent with the rigid-body motions. The compatibility of displacements at the contact area S between the soil and the rigid foundation leads to the matrix equation,

$$\{u\} = [R]\{\Delta\} \tag{8}$$

where

$$[R] = \begin{bmatrix} 1 & 0 & 0 & 0 & z & y \\ 0 & 0 & 0 & -z & 0 & x \\ 0 & 0 & 1 & y & -x & 0 \end{bmatrix} \tag{9}$$

denotes the transformation matrix; $\{\Delta\} = \{\Delta_x \quad \Delta_y \quad \Delta_z \quad \Phi_x \quad \Phi_y \quad \Phi_z\}^T$ denotes the displacement vector; and $\Delta_i \ (i = x, y, z)$ represents the translations and $\Phi_i \ (i = x, y, z)$ the rotations (see Figure 1).

If $\{P\}$ denotes the vector of loads applied to the foundation, the equilibrium between the loads applied and the forces (or tractions) distributed over the elements discretizing the volume of the foundation is expressed by the following equation:

$$\{P\} = [R]^T \{t\} \tag{10}$$

On combining Equations (7), (8) and (10), we obtain the following equation:

$$\{P\} = \left([R]^T [G]^{-1} [R]\right)\{\Delta\} = [K(\omega)]\{\Delta\} \tag{11}$$

with ω denoting the circular frequency of vibration and $[K(\omega)]$ the impedance or dynamic-stiffness matrix of the rigid foundation.

Considering the incident plane SH, P, SV and R harmonic waves to be characterized by the vertical and horizontal angles of incidence, θ_V and θ_H, respectively, as shown in Figure 1, the motion of the half-space due to these seismic waves is expressed by the following equation:

$$\{u^f\} = \{U^f\} e^{\frac{-i\omega}{c}(x\cos\theta_H + y\sin\theta_H)} \tag{12}$$

Here, $\{U^f\} = \{U_x^f \quad U_y^f \quad U_z^f\}^T$ is known as the vector of amplitudes of the soil, which depends on the z coordinate if we want to study the case of embedded foundations. However, in the case of surface foundations (i.e., $z = 0$), this is known as the vector of the amplitudes of free-field displacements. Further, c denotes the apparent velocity of the incident waves, having the form $c = c_1/\cos\theta_V$ or $c = c_2/\cos\theta_V$ for P- or S-waves, respectively, and being equal to that for the R-wave. The explicit expressions of the vector $\{U^f\}$ for the SH-, P-, SV- and R-waves are given in Wong and Luco (1978).

The presence of a rigid foundation on the surface of the half-space results in the diffraction of the above waves so that the total displacement field $\{u\}$ is expressed by the equation,

$$\{u\} = \{u^f\} + \{u^s\} \tag{13}$$

where $\{u^s\}$ represents the scattered wave field in accordance with Equation (7). Also, the total displacement field in the contact region between the foundation and the half-space must be equal to the rigid-body motion of the foundation. On substituting Equation (8) into Equation (13), written in terms of the scattered field, the force-displacement relation is obtained as

$$\{u^s\} = [R]\{\Delta\} - \{u^f\} \tag{14}$$

This may be written in terms of the traction forces by describing the scattered wave field as in Equation (7), i.e.,

$$[G]\{t\} = [R]\{\Delta\} - \{u^f\} \tag{15}$$

which then leads to

$$\{t\}=[G]^{-1}[R]\{\Delta\}-[G]^{-1}\{u^f\} \tag{16}$$

On multiplying both sides of this equation by the transpose of the transformation matrix, we obtain

$$[R]^T\{t\}=[R]^T[G]^{-1}[R]\{\Delta\}-[R]^T[G]^{-1}\{u^f\} \tag{17}$$

Combining this with Equations (10) and (11) yields the external forces. The equilibrium between external forces and seismic forces can thus be described as follows:

$$\{P\}=[K]\{\Delta\}-[K^*]\{U^f\} \tag{18}$$

where

$$[K^*]=[R]^T[G]^{-1}e^{-i\omega(x\cos\theta_H+y\sin\theta_H)/c} \tag{19}$$

is the driving force matrix.

Equation (14) can be replaced by the alternative form,

$$\{\Delta\}=[C]\{P\}+[S^*]\{U^f\} \tag{20}$$

where $[C]$ (= $[K]^{-1}$) is the dynamic compliance matrix and $[S^*]$ is the input motion matrix given by the following expression:

$$[S^*]=[C][K^*] \tag{21}$$

When the rigid foundation is acted upon by the seismic waves only, the external forces are zero (i.e., $\{P\}$ = 0), and the seismic response of the foundation is obtained from Equation (18) or (20) by using the following expression:

$$\{\Delta\}=[S^*]\{U^f\} \tag{22}$$

with

$$[S^*]=\begin{bmatrix} S_{xx} & 0 & 0 \\ 0 & S_{yy} & S_{yz} \\ 0 & S_{zy} & S_{zz} \\ 0 & R_{xy} & S_{xz} \\ R_{yx} & 0 & 0 \\ S_{zx} & 0 & 0 \end{bmatrix} \tag{23}$$

When the mass of the foundation is not zero, one simply has to replace $[K]$ by $[K]-\omega^2[M]$ in the above equations, where $[M]$ is the mass matrix of the foundation.

VALIDATION OF THE METHOD

The accuracy of the BEM-TLM method used to study the three-dimensional response of foundations subjected to plane-harmonic waves with variable angles of incidence and frequencies of vibration is validated in this section through comparisons with the results obtained by Luco and Wong (1977) and Qian and Beskos (1996) for a semi-infinite ground. A parametric study is conducted to define the parameters of the calculation model. The influence of the discretization of the soil-foundation interface is studied. The thickness of a sublayer is taken small enough for the discrete model to transmit waves in an appropriate manner and without numerical distortions. This depends on the frequencies involved and the velocity of wave propagation. The frequency of loading and velocity of wave propagation affect the precision of the numerical solution. Kausel and Peek (1982) showed that the thickness of sublayer must be smaller than a quarter of the wavelength λ. Consequently, the maximum dimensionless frequency must not exceed $N/4$, where N represents the number of sublayers.

Consider a rigid, massless, square foundation of the side $B_x = 2a$ on the surface of the half-space with a Poisson's ratio ν = 1/3, such that it is subjected to the plane P, SV and SH harmonic waves with θ_H = 90° and θ_V = 45°. Figure 4 shows the variations of the real and imaginary parts of the coefficient S_{xx} of movement with the dimensionless frequency $a_0 = \omega B/2C_s$. It is seen that the results obtained by the proposed method are in agreement with those obtained by Qian and Beskos (1996). On considering the same foundation when it is subjected to a horizontally incident Rayleigh wave (i.e., θ_H = 0°) and the corresponding velocity is taken as c_R = 0.9325c for the Poisson's ratio ν = 1/3, Figure 5 shows the real and imaginary parts of the dimensionless displacement Δ_x/R_H as functions of the frequency a_0. These results based on the BEM-TLM method are seen to be in agreement with those of Qian and Beskos (1996) and Luco and Wong (1977) based on the BEM method, except for the differences for the dimensionless frequency a_0 higher than 2.5. These differences can be explained in following two ways:

1. Qian and Beskos (1996) have used isoparametric elements to determine the soil-foundation interface. These types of elements are more accurate than the constant elements used by the method proposed in this paper.
2. Qian and Beskos (1996) and Luco and Wong (1977) have used Green's functions of a semi-infinite soil, whereas the proposed method is based on Green's functions of a soil bounded by bedrock.

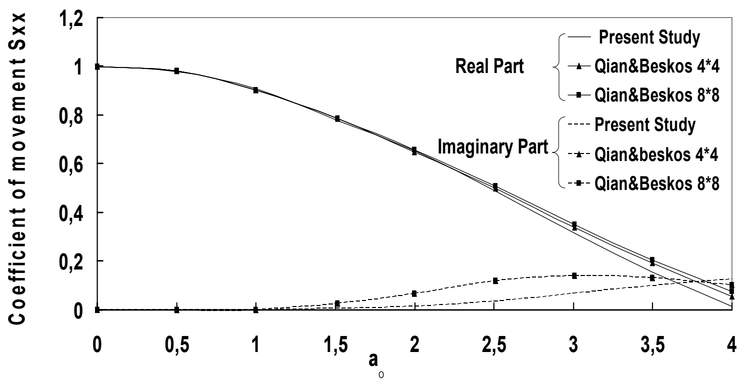

Fig. 4 Variation of coefficient S_{xx} of movement with dimensionless frequency a_0 for square foundation, $\theta_H = 0°$, $\theta_V = 45°$ and $c_s/c = 0.70711$

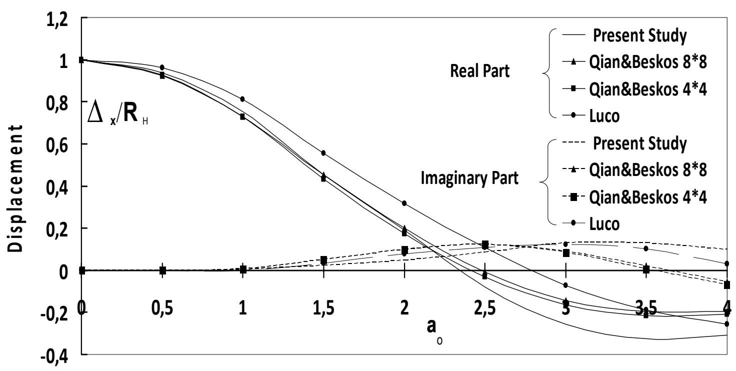

Fig. 5 Displacement response of square foundation under Rayleigh wave for $c_R/c = 0.9325$

PARAMETRIC STUDY AND DISCUSSION

1. Surface Foundation

In this section, a parametric analysis is performed for a square foundation of the side $B_x = 2a$ and subjected to the plane-harmonic waves with variable angles of incidence and frequencies of vibration (see Figure 1). The results are presented in terms of the coefficients of motion as functions of the dimensionless frequency $a_0 = \omega B/2C_s$. The soil is characterized by the height $H_t = 10$ m of the bedrock (to simulate a semi-infinite soil medium), Poisson's ratio ν = 1/3, coefficient of hysteretic damping β = 0.05, shear modulus μ = 1 and density ρ = 1 g/cm^3. The terms of the coefficient of motion are presented in the figures below for the case of S-wave with the horizontal angle of incidence $\theta_H = 90^\circ$ and the vertical angle of incidence $\theta_V = 0^\circ, 30^\circ, 45^\circ, 60^\circ$ and 90°.

1.1 Coefficients of Movements in Translation

For an angle of incidence $\theta_V = 90^\circ$, the coefficients of translational movement, S_{xx}, S_{yy}, S_{zz}, are equal to unity for all the frequencies. Typically, this value is adopted in the study of a structure subjected to the seismic loading. This value induces oversized foundations. Figures 6 and 7 show that for other angles these coefficients vary with the dimensionless frequency. The amplitude of response also depends on the vertical angle of incidence. Further, it is seen that the real parts of S_{xx} and S_{zz} have higher magnitudes than the values of the imaginary parts. At low frequencies, the response is found to be in phase with the free-field motion. These coefficients filter low frequencies and therefore behave as low-pass filters.

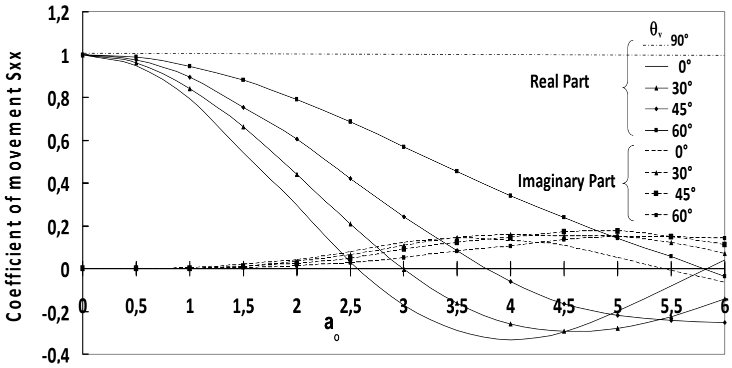

Fig. 6 Variation of coefficient S_{xx} of movement with dimensionless frequency a_0 for $\theta_H = 90^\circ$

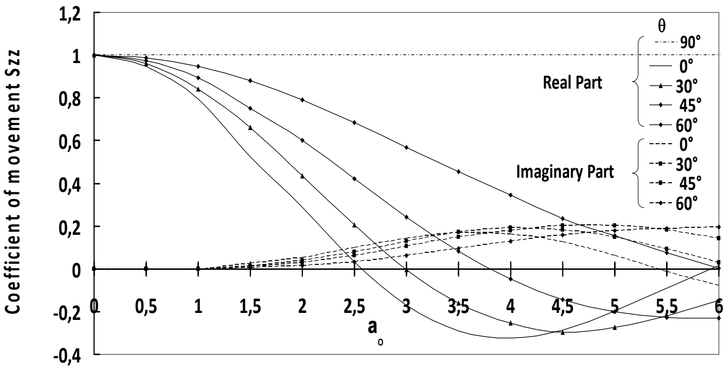

Fig. 7 Variation of coefficient S_{zz} of movement with dimensionless frequency a_0 for $\theta_H = 90^\circ$

1.2 Coefficients of Movements in Rotation and Torsion

Figures 8 and 9 present the relative coefficients of the rotational movements, R_{xy} and R_{yx}, about the x-axis and y-axis, respectively. These coefficients are zero for an angle of incidence $\theta_V = 90^\circ$ and maximum for $\theta_V = 0^\circ$. Figure 10 shows the relative coefficient of torsion, S_{zx}, about the *z*-axis as a function of dimensionless frequency for the vertical angle of incidence $\theta_V = 0^\circ, 30^\circ, 45^\circ$ and 60°. These results show that the value of the imaginary part of S_{zx} is dominant. Thus, there is a large damping in the system. Also, the response is out of phase with the free-field motion at the center of the foundation. Figures 8–10 also show that these coefficients vary with the the vertical angle of incidence θ_V, depending on the dimensionless frequency. Further, the amplitude of response depends on the vertical angle of incidence. The coefficients of movements of rotation and torsion filter high frequencies and therefore behave as high-pass filters.

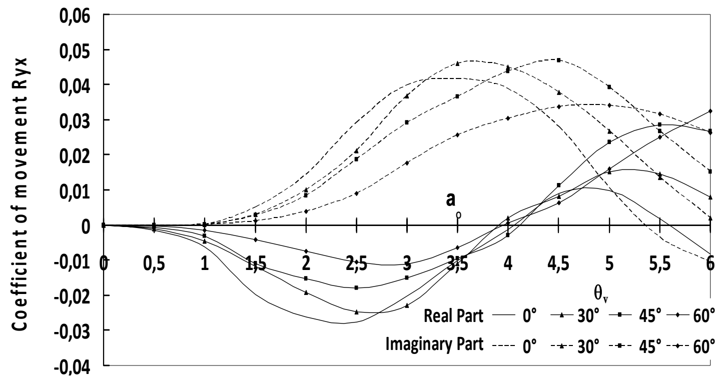

Fig. 8 Variation of coefficient R_{yx} of movement with dimensionless frequency a_0 for $\theta_H = 90°$

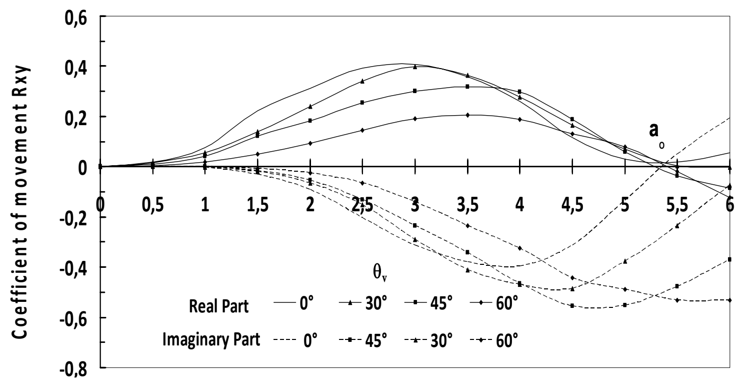

Fig. 9 Variation of coefficient R_{xy} of movement with dimensionless frequency a_0 for $\theta_H = 90°$

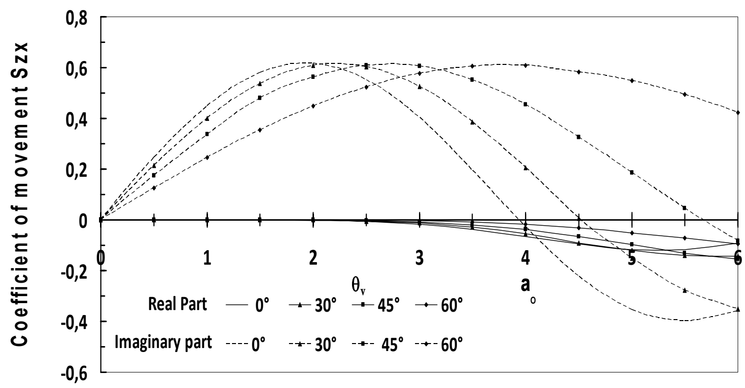

Fig. 10 Variation of coefficient S_{zx} of movement with dimensionless frequency a_0 for $\theta_H = 90°$

It may be mentioned that the matrix coefficients of movement shown in Figures 7–10 are valid only for θ_H = 90°, i.e., for S-waves with a horizontal angle of incidence. These coefficients can also be determined for other incidence angles and for other types of waves.

2. Embedded Foundation

In order to present results that are easier to understand visually, the driving-force vectors are converted to input-motion vectors by multiplying those with the inverse of the impedance matrix. Three different sets of results are given. The response of the massless foundation to the incident SH-, P- and

SV-type body waves is considered. Further, a square base of $B_x = 2a$ dimension, embedded in a homogeneous viscoelastic soil to the depth d, and subjected to the P-, SV- and SH-waves is considered (see Figure 11). The influence of the embedment ratio t ($= d/a$, taken as equal to 0, 0.3 and 0.6) on the seismic response of the foundation is studied. The results are presented in terms of displacements, rotations and torsion; these terms are calculated by using Equation (18) as the functions of the dimensionless frequency a_0. In order to simplify the presentation in this paper, only one direction of wave propagation is considered with the vertical incident angle θ_V taken as 45°. Figures 12–19 represent the terms of displacement, rotation and torsion caused by the incident P-, SV- and SH-waves. These curves are given for different values of relative embedment.

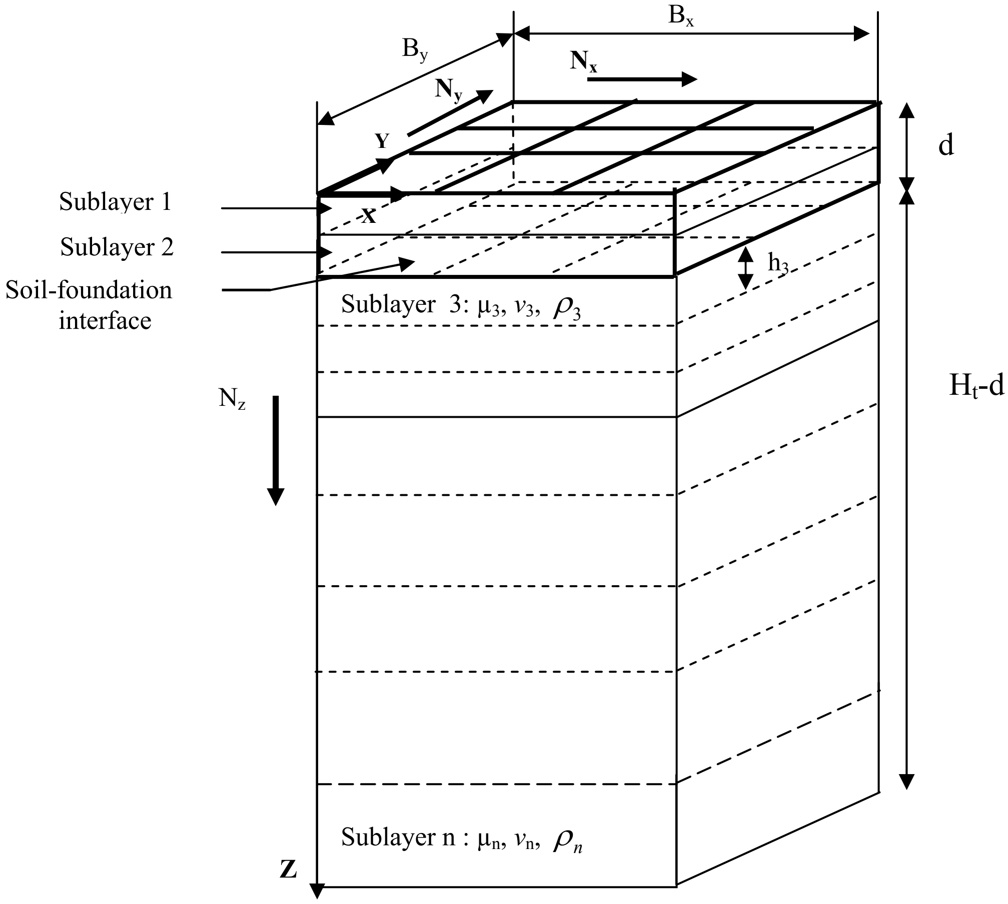

Fig. 11 Model of calculation for an embedded foundation subjected to harmonic seismic waves

2.1 Compression or P-Wave

The response of a massless foundation to an incident P-wave is considered. The wave travels in the x-direction with the particle motion taking place in the z- and x-directions. Except for the vertical incidence, i.e., θ_V = 90°, the incident P-wave causes a mode conversion, thus resulting in a reflected SV-wave. One angle of incidence is considered, which is equal to 45° (with respect to the x-axis). The wavelength of the incident P-wave is twice as long as that of the incident S-waves; therefore, the kinematic interaction now is less prominent. In general, the P-wave induces displacements along the x- and z-axes and rotation around the y-axis. Figures 12–14 respectively show the variations of displacements and rotation as the functions of dimensionless frequency, with the embedment coefficient t taken as 0, 0.3 and 0.6.

It may be observed that the displacements Δ_x and Δ_z and the rotation ϕ_y are strongly attenuated due to an increase in the embedment. Further, the horizontal displacement Δ_x is affected more by the embedment than the vertical displacement Δ_z and rotation ϕ_y. It is seen that on increasing the embedment, the displacements and rotation are cancelled as the frequency decreases and then the signs change. The imaginary parts of the vertical and horizontal modes of translation are not affected by an increase in the embedment. In contrast, the imaginary part of the rotation is strongly affected by the embedment.

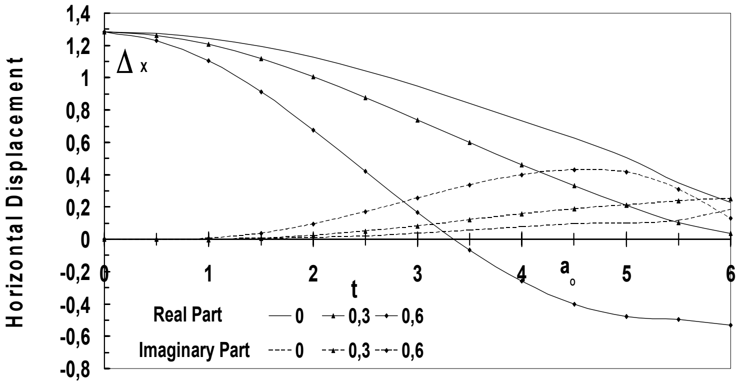

Fig. 12 Variations of horizontal input motion Δ_x due to incident P-wave with a_0 for $\theta_V = 45°$ and $\theta_H = 0°$

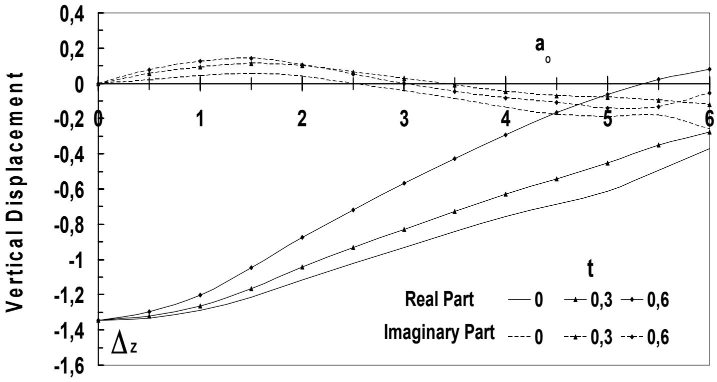

Fig. 13 Variations of horizontal input motion Δ_z due to incident P-wave with a_0 for $\theta_V = 45°$ and $\theta_H = 0°$

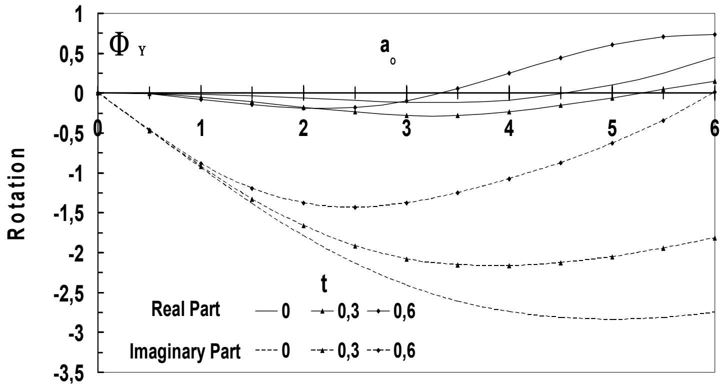

Fig. 14 Variations of rocking input motion ϕ_y due to incident P-wave with a_0 for $\theta_V = 45°$ and $\theta_H = 0°$

2.2 SV-Wave

The response of a massless foundation subjected to an incident SV-wave is considered. The wave travels in the x-direction with its particle motion in the z- and x-directions. For the vertical incident angle θ_V taken as 45°, the free-field motion for the SV-wave in the direction of propagation is zero. Further, similar to the case of P-wave, only the horizontal, vertical, and rocking components are excited. Figures 15–17 show the variations of displacements and rotation as the functions of frequency and thus show the influence of embedment on the motion of the foundation. Figure 15 shows that the displacement Δ_x is zero for a foundation on the surface (with t = 0). This, however, becomes non-zero for the relative embedment of t = 0.3 and 0.6, with the imaginary part getting strongly affected, and thus the foundation does not follow the free-field motion. Moreover, the horizontal displacement Δ_x is more affected by the presence of embedment than the vertical displacement Δ_z and the rotation ϕ_y, especially at low frequencies. The presence of embedment in the foundation just changes the signs of vertical displacement and rotation for the frequency a_0 greater than 4.

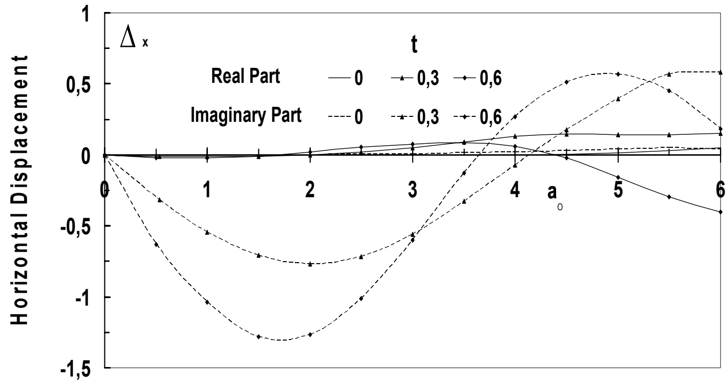

Fig. 15 Variations of horizontal input motion Δ_x due to incident SV-wave with a_0 for $\theta_V = 45°$ and $\theta_H = 0°$

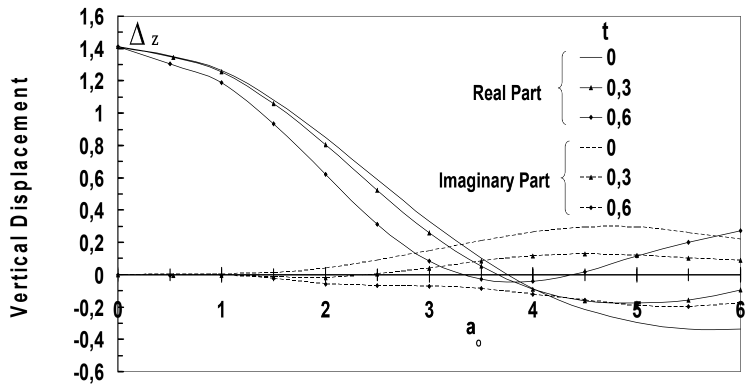

Fig. 16 Variations of vertical input motion Δ_z due to incident SV-wave with a_0 for $\theta_V = 45°$ and $\theta_H = 0°$

2.3 SH-Wave

The response of a square, massless foundation to a SH-wave is considered, with the horizontal angle of incidence θ_H taken as 90°. The incident wave travels in the y-direction; therefore, the particle motion of the wave is in the x-direction. This wave causes displacement and torsion in the foundation as shown in Figures 18 and 19 respectively for various cases of embedment (i.e., t = 0, 0.3 and 0.6). Figures 18 and 19 show that the horizontal displacement Δ_x and torsion ϕ_z are strongly affected by the embedment of the foundation. For dimensionless frequencies lower than 3, Δ_x is not affected by increasing the relative embedment. This is however not the case for ϕ_z, which is strongly affected by an increase in the embedment. In contrast, for frequencies greater than 3, the presence of the foundation embedment causes a change in the signs of Δ_x and ϕ_z.

It is seen in all the above results for foundation embedment (see Figures 12–19) that the horizontal displacement caused by a P-wave is more attenuated than the displacement caused by a SH or SV-wave. On the other hand, the rotation caused by a SV-wave is more attenuated than the rotation caused by a P-wave.

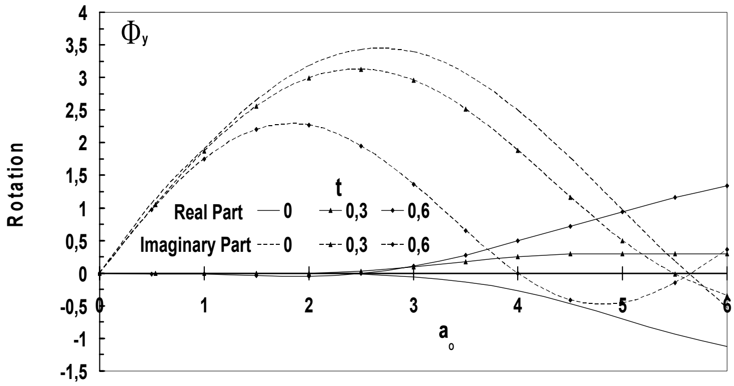

Fig. 17 Variations of rocking input motion ϕ_y due to incident SV-wave with a_0 for $\theta_V = 45°$ and $\theta_H = 0°$

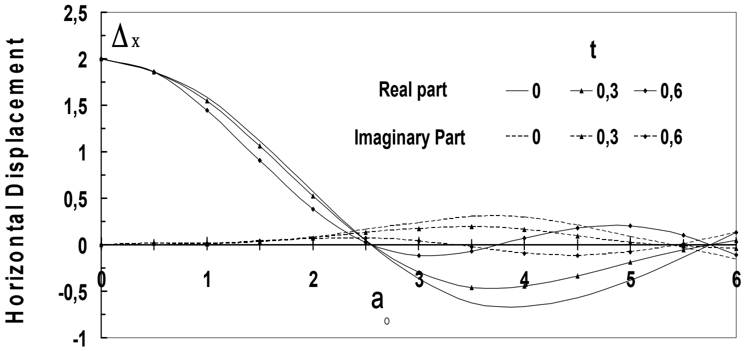

Fig. 18 Variations of horizontal input motion Δ_x due to incident SH-wave with a_0 for $\theta_V = 45°$ and $\theta_H = 90°$

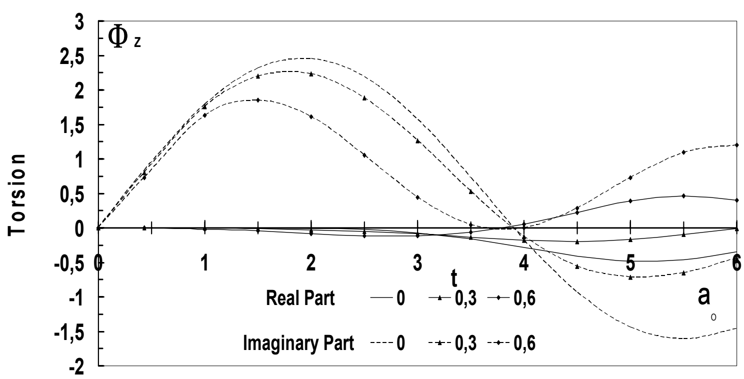

Fig. 19 Variations of torsion input motion ϕ_z due to incident SH-wave with a_0 for $\theta_V = 45°$ and $\theta_H = 90°$

CONCLUSIONS

The seismic response of a square, rigid foundation embedded in a homogeneous, viscoelastic soil and subjected to obliquely incident harmonic P-, SV-, SH- and R-waves has been formulated. A simplified BEM-TLM method has been developed and used to calculate the foundation-input motion under different travelling seismic waves. The solution has been formulated by using the boundary-element method in frequency domain while using the formalism of Green's functions. Constant quadrilateral elements have been used to obtain the seismic response based on this formulation. The efficiency of this method has been confirmed by comparison with the results of previous studies. This method is remarkably simple and has been concluded to be highly effective and economical to determine input motions for the rigid foundations of arbitrary geometry. The originality of the method lies first in the insignificance of the number of elements used in the discretization of the model and second in its ability to simulate a limited height of bedrock.

This study has also highlighted the importance of the inclination of incident waves on the behavior of a foundation. The results indicate the following:

- The response of a foundation subject to non-vertical incident waves is different from that of a foundation subject to vertically incident waves.
- Non-vertical incident waves generate torsion, translation, and rotation in the foundation, while vertically incident waves cause translation only.
- Assuming vertical angle of incidence (i.e., $\theta_V = 0^{\circ}$) leads to an oversizing of the foundations.
- The coefficients of translational movement filter low frequencies, while the coefficients of rotational movement filter high frequencies.
- The embedment of foundation affects displacement, rotation, and torsion in more specific ways and acts as a favorable factor in the seismic response of foundations. The movement of the foundation is strongly attenuated for foundations with relatively larger embedment depths, especially at low frequencies.

REFERENCES

1. Apsel, R.J. and Luco, J.E. (1987). "Impedance Functions for Foundations Embedded in a Layered Medium: An Integral Equation Approach", Earthquake Engineering & Structural Dynamics, Vol. 15, No. 2, pp. 213–231.
2. Aubry, D. and Clouteau, D. (1992). "A Subdomain Approach to Dynamic Soil-Structure Interaction" in "Recent Advances in Earthquake Engineering and Structural Dynamics (edited by V.E. Davidovici)", Ouest Éditions, Presses Académiques, Nantes, France.
3. Beskos, D.E. (1987). "Boundary Element Methods in Dynamic Analysis", Applied Mechanics Reviews, Vol. 40, No. 1, pp. 1–23.
4. Boumekik, A. (1985). "Fonctions Impédances d'une Fondation Vibrante en Surface ou Partiellement Encastrée dans un sol Multicouche", Ph.D. Thesis, Université Libre de Bruxelles, Brussels, Belgium (in French).
5. Çelebi, E., Fırat, S. and Çankaya, İ. (2006). "The Evaluation of Impedance Functions in the Analysis of Foundations Vibrations Using Boundary Element Method", Applied Mathematics and Computation, Vol. 173, No. 1, pp. 636–667.
6. Fujimori, T., Tsunoda, T., Izumi, M. and Akino, K. (1992). "Partial Embedment Effects on Soil-Structure Interaction", Proceedings of the Tenth World Conference on Earthquake Engineering, Madrid, Spain, Vol. 3, pp. 1713–1718.
7. Imamura, A., Watanabe, T., Ishizaki, M. and Motosaka, M. (1992). "Seismic Response Characteristics of Embedded Structures Considering Cross Interaction", Proceedings of the Tenth World Conference on Earthquake Engineering, Madrid, Spain, Vol. 3, 1719–1724.
8. Karabalis, D.L. and Mohammadi, M. (1998). "3-D Dynamic Foundation-Soil-Foundation Interaction on Layered Soil", Soil Dynamics and Earthquake Engineering, Vol. 17, No. 3, pp. 139–152.
9. Kausel, E. and Peek, R. (1982). "Dynamic Loads in the Interior of a Layered Stratum: An Explicit Solution", Bulletin of the Seismological Society of America, Vol. 72, No. 5, pp. 1459–1481.

10. Kausel, E. and Roësset, J.M. (1981). "Stiffness Matrices for Layered Soils", Bulletin of the Seismological Society of America, Vol. 71, No. 6, pp. 1743–1761.
11. Kausel, E., Whitman, R.V., Morray, J.P. and Elsabee, F. (1978). "The Spring Method for Embedded Foundations", Nuclear Engineering and Design, Vol. 48, No. 2-3, pp. 377–392.
12. Lin, H.-T. and Tassoulas, J.L. (1986). "A Hybrid Method for Three-Dimensional Problems of Dynamics of Foundations", Earthquake Engineering & Structural Dynamics, Vol. 14, No. 1, pp. 61–74.
13. Liou, G.-S. (1993). "Impedance for Rigid Square Foundation on Layered Medium", Structural Engineering/Earthquake Engineering, JSCE, Vol. 10, No. 2, pp. 83s–93s.
14. Liou, G.-S. and Chung, I.L. (2009). "Impedance Matrices for Circular Foundation Embedded in Layered Medium", Soil Dynamics and Earthquake Engineering, Vol. 29, No. 4, pp. 677–692.
15. Luco, J.E. and Wong, H.L. (1977). "Dynamic Response of Rectangular Foundations for Rayleigh Wave Excitation", Proceedings of the Sixth World Conference on Earthquake Engineering, New Delhi, Vol. II, pp. 1542–1547.
16. Lysmer, J. and Waas, G. (1972). "Shear Waves in Plane Infinite Structures", Journal of the Engineering Mechanics Division, Proceedings of ASCE, Vol. 98, No. EM1, pp. 85–105.
17. McKay, K. (2009). "Three Applications of the Reciprocal Theorem in Soil-Structure Interaction", Ph.D. Dissertation, University of Southern California, Los Angeles, U.S.A.
18. Mizuhata, K., Kusakabe, K. and Shirase, Y. (1988). "Study on Dynamic Characteristics of Embedded Mass and Its Surrounding Ground", Proceedings of Ninth World Conference on Earthquake Engineering, Tokyo-Kyoto, Japan, Vol. III, pp. 679–684.
19. Mohammadi, M. (1992). "3-D Dynamic Foundation-Soil-Foundation Interaction by BEM", Ph.D. Dissertation, Department of Civil Engineering, University of South Carolina, Columbia, U.S.A.
20. Ohtsuka, Y., Fukuoka, A., Akino, K. and Ishida, K. (1996). "Experimental Studies on Embedment Effects on Dynamic Soil-Structure Interaction", Proceedings of the Eleventh World Conference on Earthquake Engineering, Acapulco, Mexico, Paper No. 59 (on CD).
21. Pecker, A. (1984). "Dynamique des Sols", Presses de l'Ecole Nationale des Ponts et Chaussées, Paris, France (in French).
22. Qian, J. and Beskos, D.E. (1996). "Harmonic Wave Response of Two 3-D Rigid Surface Foundations", Soil Dynamics and Earthquake Engineering, Vol. 15, No. 2, pp. 95–110.
23. Sbartai, B. and Boumekik, A. (2006). "Vertical Compliance Function of Adjacent Surface Rigid Footings in Heterogeneous Soil Layer", Proceedings of the Sixth European Conference on Numerical Methods in Geotechnical Engineering, Graz, Austria, pp. 217–222.
24. Sbartai, B. and Boumekik, A. (2007). "Horizontal Compliance Function of Adjacent Surface Rigid Footings in Homogeneous Soil Limited by a Substratum", Proceedings of the Fourth International Conference on Earthquake Geotechnical Engineering, Thessaloniki, Greece, Paper No. 1729 (on CD).
25. Sbartai, B. and Boumekik, A. (2008). "Ground Vibration from Rigid Foundation by BEM-TLM", ISET Journal of Earthquake Technology, Vol. 45, No. 3-4, pp. 65–78.
26. Spyrakos, C.C. and Xu, C. (2004). "Dynamic Analysis of Flexible Massive Strip-Foundations Embedded in Layered Soils by Hybrid BEM-FEM", Computers & Structures, Vol. 82, No. 29-30, pp. 2541–2550.
27. Suárez, M., Avilés, J. and Sánchez-Sesma, F.J. (2002). "Response of L-Shaped Rigid Foundations Embedded in a Uniform Half-Space to Traveling Seismic Waves", Soil Dynamics and Earthquake Engineering, Vol. 22, No. 8, pp. 625–637.
28. Watakabe, M., Matsumoto, H., Ariizumi, K., Fukahori, Y., Shikama, Y., Yamanouchi, K. and Kuniyoshi, H. (1992). "Earthquake Observation of Deeply Embedded Building Structure", Proceedings of the Tenth World Conference on Earthquake Engineering, Madrid, Spain, Vol. 3, pp. 1831–1838.
29. Wong, H.L. and Luco, J.E. (1978). "Dynamic Response of Rectangular Foundations to Obliquely Incident Seismic Waves", Earthquake Engineering & Structural Dynamics, Vol. 6, No. 1, pp. 3–16.
30. Wong, H.L. and Luco, J.E. (1986). "Dynamic Interaction between Rigid Foundations in a Layered Half-Space", Soil Dynamics and Earthquake Engineering, Vol. 5, No. 3, pp. 149–158.